



The Hassania School of Public Works

Effects of Climate Change on Moroccan Coastal Upwelling: Relationships between the NAO, Upwelling Index, and Sea Surface Temperature (1978-2024)

Prepared by:

Mohammed El Abdioui

Supervised by:

Rachid Ilmen

Casablanca - Morocco
October 2025

Contents

1 General Introduction	5
1.1 Subject Context	5
1.2 Problem Statement	6
1.3 General Objective	6
1.4 Specific Objectives	7
2 Materials and Methods	8
2.1 Scientific Instruments Used	8
2.1.1 Languages and Environments	8
2.1.2 Python Scientific Libraries	8
2.1.3 Data Used	8
2.2 Methodological Approach	9
2.2.1 Calculation of Climate Indices	9
2.2.2 Statistical Analysis	11
2.2.3 Analysis of Climate Trends and Breakpoint Detection	13
3 Results and Discussion	15
3.1 Obtained Results	15
3.1.1 Variability of the NAO Index (1978-2022) and Moroccan Upwelling Context	15
3.1.2 Relationships between NAO, Upwelling and SST	17
3.1.3 Graphical and Correlation Analysis	19
3.1.4 Analysis of Climate Trends 1978-2024	21
3.1.5 Granger Causality Analysis	28
3.1.6 Climate Trends and Breakpoint Detection	30
3.1.7 Discussion and Comparison with Literature	34
3.1.8 Synthesis of Causal Relationships	35
3.1.9 Socio-economic Implications	35
4 General Conclusion and Perspectives	37
4.1 Synthesis of Main Results	37

4.1.1	Seasonal variability of ocean-atmosphere relationships	37
4.1.2	North-south spatial gradient	37
4.1.3	Climate trends 1978-2024	37
4.1.4	Upwelling mapping	38
4.1.5	Granger causality analysis	38
4.2	Validation with Literature	38
4.3	Environmental and Socio-economic Implications	38
4.3.1	Impacts on fishing	38
4.3.2	Regional climate paradox	39
4.3.3	Other sectors	39
4.4	Study Limitations	39
4.5	Research Perspectives	39
4.6	Final Conclusion	40

List of Figures

1.1	Geographic representation of the Atlantic coast of Morocco, indicating the main coastal cities studied along the coastline, from Dakhla to Tangier. The coastlines of neighboring countries are included to provide regional context, with Lisbon (Portugal) used as a reference point.	6
3.1	Monthly and seasonal evolution of the NAO index (1978-2022). Colors represent seasons: DJF (blue), MAM (green), JJA (red), SON (orange).	15
3.2	Seasonal evolution of normalized indices of NAO (blue), upwelling (green), and SST (red) along the Moroccan Atlantic coast between 1978 and 2024. Marked interannual variability is observed, particularly in winter (DJF) and summer (JJA), reflecting differentiated seasonal influence of NAO on upwelling intensity and sea surface temperature.	19
3.3	Correlation matrices between NAO, Upwelling and SST indices for each season. Positive correlations (red) indicate direct relationships, while negative correlations (blue) indicate inverse relationships.	20
3.4	Analysis of seasonal climate trends (1978-2024) for NAO, Upwelling and SST indices. Graphs show temporal evolution with linear trends (dotted lines) and corresponding regression equations. Trends are expressed in units per decade, with indication of statistical significance (* for $p < 0.05$).	22
3.5	Seasonal correlation between sea surface temperature (SST) and NAO index along the Moroccan Atlantic coast. Hatched areas indicate statistical significance ($p < 0.05$). Negative correlations dominate, with visible north-south latitudinal gradient, particularly strong in MAM south of Casablanca.	25
3.6	Seasonal correlation between coastal upwelling index (CUI) and SST. Hatching: significance ($p < 0.05$). Negative correlations indicate cooling associated with upwelling, with maximum in SON (cumulative effect) and JJA (summer peak) off Safi-Essaouira.	26
3.7	Spatial analysis of Granger causality. Top: CUI → SST (JJA); Middle: NAO → SST (SON); Bottom: SST → NAO (SON). Columns: F-statistic, ΔR^2 , optimal lag (months). Red contours: significance.	28

3.8 Trends of sea surface temperature (SST) along the Moroccan Atlantic coast (1978-2024). The map shows generalized warming (+0.149°C/decade on average) with 98.2% of the area warming and only 1.8% cooling. Hatched areas indicate statistical significance ($p < 0.05$).	31
3.9 Breakpoints detected in seasonal climate index time series (1978-2024). Dotted vertical lines indicate years of climate regime change detected automatically. . .	32
3.10 Annual mean magnitude of upwelling transport (Ekman Transport) along the Moroccan Atlantic coast (1978-2024). Color indicates intensity, and curves (blue, green, red) represent dynamic classification thresholds based on percentiles of calculated data (P25, P50, P75).	33

Chapter 1

General Introduction

1.1 Subject Context

Climate change currently represents one of the greatest environmental challenges on a global scale. Its effects are particularly evident in coastal areas, where interactions between the atmosphere, ocean, and biosphere influence marine ecosystem dynamics.

Among the ocean processes most sensitive to these changes is **coastal upwelling**, a phenomenon where deep, cold, nutrient-rich waters rise to the surface, thus stimulating biological productivity and regulating regional climate.

The **Moroccan Atlantic coast**, stretching approximately 3500 km and representing one of the world's most dynamic upwelling zones, constitutes a privileged study area for assessing the impact of global warming on ocean-atmosphere processes. The intensity and variability of this upwelling directly influence fishery resources and, consequently, local economic activities such as:

- **Artisanal fishing**, characterized by small traditional boats (barques) and local practices, which heavily depends on fish availability near the coastline.
- **Industrial fishing**, more industrial and destined for export or national markets, which exploits resources further out at sea and contributes significantly to the national economy.

Today, the Moroccan climate is characterized by **structural drought**, which has induced a **shift in rainfall patterns** across the national territory, leading to **spatio-temporal variation in precipitation** across the country. These climatic conditions increase the sensitivity of coastal ecosystems and economic sectors dependent on marine resources.

In this context, the joint analysis of the **NAO**, the **Coastal Upwelling Index (CUI)**, and **Sea Surface Temperature (SST)** over a long period (1978-2024) allows for a better understanding of trends, climate variability mechanisms, and their potential impacts on coastal ecosystems and economic sectors related to fishing along the Moroccan coast. This study focuses specifically on

the 3500 km of the Atlantic coastline, to provide a comprehensive view of the spatio-temporal variability of upwelling and its effects on artisanal and industrial fishing.

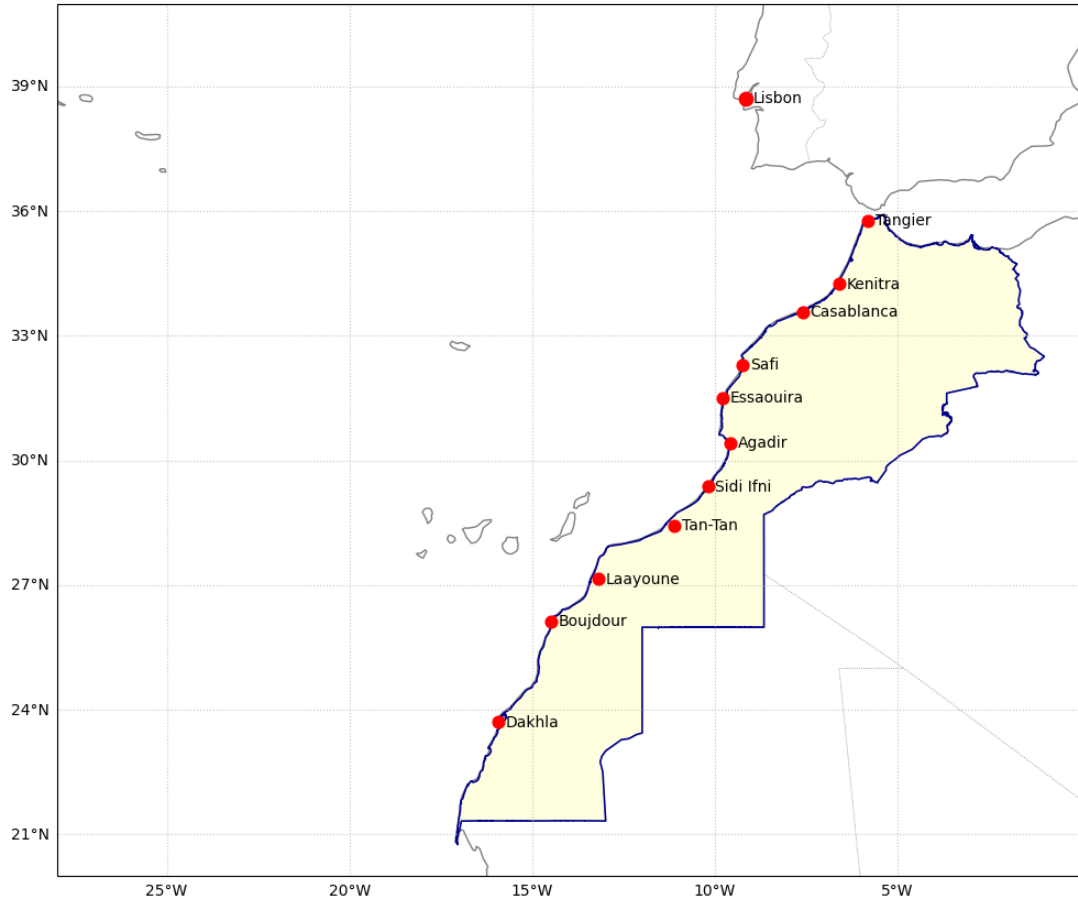


Figure 1.1: Geographic representation of the Atlantic coast of Morocco, indicating the main coastal cities studied along the coastline, from Dakhla to Tangier. The coastlines of neighboring countries are included to provide regional context, with Lisbon (Portugal) used as a reference point.

1.2 Problem Statement

How do climate change and atmospheric variability, represented by the North Atlantic Oscillation (NAO), influence the dynamics of upwelling along the Moroccan Atlantic coast? And what are the potential consequences for sea surface temperature, marine productivity, coastal ecosystems, and dependent socio-economic activities such as fishing, aquaculture, and coastal tourism?

1.3 General Objective

This work aims to **analyze the impact of climate change and atmospheric variability on the dynamics of Moroccan coastal upwelling**, to better understand the interactions between the atmosphere and the ocean in the context of global warming.

1.4 Specific Objectives

More specifically, the objectives are to:

1. Analyze the temporal evolution of CUI, SST, and NAO over the period 1978-2024;
2. Study correlations between these variables to identify dominant trends and associated climate regimes;
3. Assess the influence of climate change on the intensity and seasonality of Moroccan upwelling;
4. Highlight the environmental and socio-economic implications of these evolutions, particularly on marine productivity and dependent sectors such as fishing and coastal tourism.

Chapter 2

Materials and Methods

2.1 Scientific Instruments Used

This study was conducted using the following software tools and programming environments:

2.1.1 Languages and Environments

- **Python 3.9**: Main programming language for data analysis and scientific computations
- **Jupyter Notebook**: Interactive development environment for prototyping and exploratory analysis

2.1.2 Python Scientific Libraries

- **xarray (v0.20.1)** and **netCDF4 (v1.6.2)**: Reading and manipulation of NetCDF files containing ERA5 data
- **NumPy (v1.23.0)** and **pandas (v1.5.0)**: Numerical computations and tabular data processing
- **SciPy (v1.9.0)**: Statistical analyses and advanced scientific functions
- **statsmodels (v0.13.2)**: Implementation of Granger causality tests and other temporal analyses
- **Matplotlib (v3.6.0)** and **Seaborn (v0.12.0)**: Data visualization and graph creation

2.1.3 Data Used

The data used in this study come from the **ERA5 reanalysis** produced by the *European Centre for Medium-Range Weather Forecasts* (ECMWF). They were obtained via the Copernicus Climate Data Store (CDS) portal.

- **Product type:** Monthly averaged reanalysis
- **Variables used:**
 - 10m u-component of wind
 - 10m v-component of wind
 - Mean sea level pressure (SLP)
 - Sea surface temperature (SST)
- **Temporal period:** 1978-2024 (42 continuous years of data)
- **Temporal resolution:** Monthly data
- **Spatial resolution:** ERA5 grid at $0.25^\circ \times 0.25^\circ$ (approximately 28 km), covering the entire North Atlantic, including the Moroccan Atlantic coast
- **File format:** Uncompressed NetCDF4 (Experimental)

These data offer essential spatio-temporal consistency for studying interactions between the atmosphere and the ocean. The selected variables allow examination of the physical mechanisms governing the **variability of Moroccan coastal upwelling**, in relation to the **North Atlantic Oscillation (NAO)** and **sea surface temperature (SST)** over the period 1978-2024, the main analysis period used in this work.

2.2 Methodological Approach

2.2.1 Calculation of Climate Indices

NAO Index

The NAO index was calculated according to the standard approach based on normalized pressure difference between the Azores (37°N - 23°W) and Iceland (65°N - 22°W):

1. Extraction of SLP data at representative grid points
2. Calculation of anomalies relative to the reference period 1981-2010
3. Monthly normalization of anomalies to eliminate seasonal effects
4. Calculation of normalized difference:

$$NAO = \frac{P_{\text{Azores}} - \mu_{\text{Azores}}}{\sigma_{\text{Azores}}} - \frac{P_{\text{Iceland}} - \mu_{\text{Iceland}}}{\sigma_{\text{Iceland}}} \quad (2.1)$$

Upwelling Index

The Moroccan coastal upwelling index was calculated according to the formulation by Hilmi et al. (2022):

$$M_x = \frac{\rho_{\text{air}} C_d |V| u_{10}}{\rho_w f} \quad (2.2)$$

$$M_y = \frac{\rho_{\text{air}} C_d |V| v_{10}}{\rho_w f} \quad (2.3)$$

$$UI = -M_y \times 100 \quad (2.4)$$

where:

- $\rho_{\text{air}} = 1.22 \text{ kg m}^{-3}$, $\rho_w = 1025 \text{ kg m}^{-3}$
- $C_d = 1.4 \times 10^{-3}$ (drag coefficient)
- $f = 2\omega \sin(\varphi)$ (Coriolis parameter)
- u_{10}, v_{10} : zonal and meridional components of wind at 10 m

Ekman Transport

The offshore Ekman transport (Q_E) was calculated to quantify water volume transported perpendicular to the coast:

$$\tau_x = \rho_{\text{air}} C_d u_{10} \sqrt{u_{10}^2 + v_{10}^2} \quad (2.5)$$

$$\tau_y = \rho_{\text{air}} C_d v_{10} \sqrt{u_{10}^2 + v_{10}^2} \quad (2.6)$$

$$Q_{E_x} = \frac{\tau_y}{\rho_w f} \quad (2.7)$$

$$Q_{E_y} = -\frac{\tau_x}{\rho_w f} \quad (2.8)$$

$$|Q_E| = \sqrt{Q_{E_x}^2 + Q_{E_y}^2} \quad (2.9)$$

where τ_x, τ_y are wind stress components (N/m^2). The upwelling index (UI) is equivalent to $-Q_{E_y} \times 100$.

2.2.2 Statistical Analysis

Data Preprocessing

- Normalization of time series:

$$X_{\text{norm}} = \frac{X - \mu}{\sigma} \quad (2.10)$$

- Seasonal aggregation according to meteorological seasons:

- Winter (DJF): December, January, February
- Spring (MAM): March, April, May
- Summer (JJA): June, July, August
- Autumn (SON): September, October, November

Granger Causality Analysis

The Granger causality test procedure between the NAO index, upwelling, and SST follows the methodology established by Kaufmann and Stern (1997). This approach includes two main steps and allows identification of the presence and direction of causal relationships.

VAR Modeling In the first step, interactions between NAO, upwelling, and SST anomalies are described using a vector autoregressive (VAR) model. For each variable pair, the equation system is written:

$$\text{NAO}_t = \alpha_1 + \sum_{i=1}^s \beta_{1i} \text{NAO}_{t-i} + \sum_{i=1}^s \gamma_{1i} \text{SST}_{t-i} + \epsilon_{1t} \quad (2.11)$$

$$\text{SST}_t = \alpha_2 + \sum_{i=1}^s \beta_{2i} \text{NAO}_{t-i} + \sum_{i=1}^s \gamma_{2i} \text{SST}_{t-i} + \epsilon_{2t} \quad (2.12)$$

Similarly, for relationships between upwelling and SST:

$$\text{UI}_t = \alpha_3 + \sum_{i=1}^s \beta_{3i} \text{UI}_{t-i} + \sum_{i=1}^s \gamma_{3i} \text{SST}_{t-i} + \epsilon_{3t} \quad (2.13)$$

$$\text{SST}_t = \alpha_4 + \sum_{i=1}^s \beta_{4i} \text{UI}_{t-i} + \sum_{i=1}^s \gamma_{4i} \text{SST}_{t-i} + \epsilon_{4t} \quad (2.14)$$

where α , β , and γ are regression coefficients, ϵ represents error terms, and s is the lag length determined by a likelihood ratio test (Sims, 1980).

Seasonal Specification To account for seasonal variability in ocean-atmosphere interactions, we adapted the basic VAR equations for each meteorological season (DJF, MAM, JJA, SON). For example, for winter:

$$\text{NAOWinter}_t = \alpha_1 + \sum_{i=1}^s \beta_{1i} \text{NAOWinter}_{t-i} + \sum_{i=1}^s \gamma_{1i} \text{SST}_{\text{Winter}_{t-i}} + \epsilon_{1t} \quad (2.15)$$

$$\text{SST}_{\text{Winter}_t} = \alpha_2 + \sum_{i=1}^s \beta_{2i} \text{NAOWinter}_{t-i} + \sum_{i=1}^s \gamma_{2i} \text{SST}_{\text{Winter}_{t-i}} + \epsilon_{2t} \quad (2.16)$$

Causality Test To determine the direction of causality, we estimate restricted forms of the equations by eliminating the potential causal variable. For example, to test if SST causes NAO variability, we estimate the restricted equation:

$$\text{NAO}_t = \alpha'_1 + \sum_{i=1}^s \beta'_{1i} \text{NAO}_{t-i} + \epsilon'_{1t} \quad (2.17)$$

Test Statistic Statistical significance is evaluated using an F-statistic calculated as:

$$F = \frac{(RSS_r - RSS_u)/s}{RSS_u/(T - k)} \quad (2.18)$$

where:

- RSS_r and RSS_u are residual sums of squares of restricted and unrestricted models
- s is the number of coefficients restricted to zero
- T is the number of observations
- k is the total number of regressors in the unrestricted model

Complementary Causality Measure In addition to the F-statistic, we calculate the difference in coefficients of determination (ΔR^2) to quantify the improvement in variance explanation:

$$\Delta R^2 = R_u^2 - R_r^2 = \frac{RSS_r - RSS_u}{RSS_r} \quad (2.19)$$

where:

- $R_u^2 = 1 - \frac{RSS_u}{TSS}$ is the coefficient of determination of the unrestricted model
- $R_r^2 = 1 - \frac{RSS_r}{TSS}$ is the coefficient of determination of the restricted model
- TSS is the total sum of squares

This ΔR^2 measure represents the additional proportion of variance explained by including lags of the causal variable in the model.

Interpretation A statistically significant F-value (threshold $p < 0.05$) rejects the null hypothesis of non-causality. This indicates that lagged values of the eliminated variable contain unique information for predicting the dependent variable, beyond that contained in its own past values.

The F-statistic evaluates whether the improvement in fit due to including additional lags is statistically significant, while ΔR^2 quantifies the practical magnitude of this improvement in terms of explained variance.

In our study, this procedure was systematically applied to all variable pairs (NAO-SST, Upwelling-SST, NAO-Upwelling) and for each season, with a maximum lag number $s = 2$ determined as optimal by Akaike (AIC) and Bayesian (BIC) information criteria. The combined results of the F-statistic and ΔR^2 allow robust interpretation of causal relationships, distinguishing both statistical significance and practical importance of identified relationships.

2.2.3 Analysis of Climate Trends and Breakpoint Detection

Calculation of Linear Trends

To quantify the impact of climate change on the studied variables, we calculated linear trends per decade for each season and each variable (NAO, Upwelling, SST) over the period 1978-2024. The methodology employed is as follows:

1. Extraction of normalized seasonal data from existing CSV files
2. Application of linear regression for each variable and each season:

$$y = ax + b \quad (2.20)$$

3. Conversion of slope (a) to units per decade:

$$a_{\text{decade}} = a \times 10 \quad (2.21)$$

4. Test of statistical significance (threshold $p < 0.05$) via Student's t-test

SST Trend Mapping

A spatial analysis of sea surface temperature trends was conducted to identify warming and cooling zones along the Moroccan coastline:

- Calculation of linear trend for each pixel of the ERA5 grid (0.25°)

- Annual aggregation of SST data (average over 12 months)
- Application of linear regression pixel by pixel
- Statistical masking ($p < 0.05$) to retain only significant trends

Breakpoint Detection

Change point analysis was used to identify abrupt changes in climatic time series:

- Use of the `BinSeg` (Binary Segmentation) algorithm from the `ruptures` package
- Preliminary normalization of time series
- Automatic detection of optimal number of breakpoints
- Visual validation of detected breakpoints

This approach allows identification of key years where climate regimes changed significantly.

Chapter 3

Results and Discussion

3.1 Obtained Results

3.1.1 Variability of the NAO Index (1978-2022) and Moroccan Upwelling Context

Analysis of the temporal evolution of the NAO (North Atlantic Oscillation) index reveals marked interannual variability with alternating positive and negative phases (Figure 3.1). Variability is most pronounced in winter (DJF - December-January-February) with a standard deviation of 0.909, compared to 0.353 in summer (JJA - June-July-August).

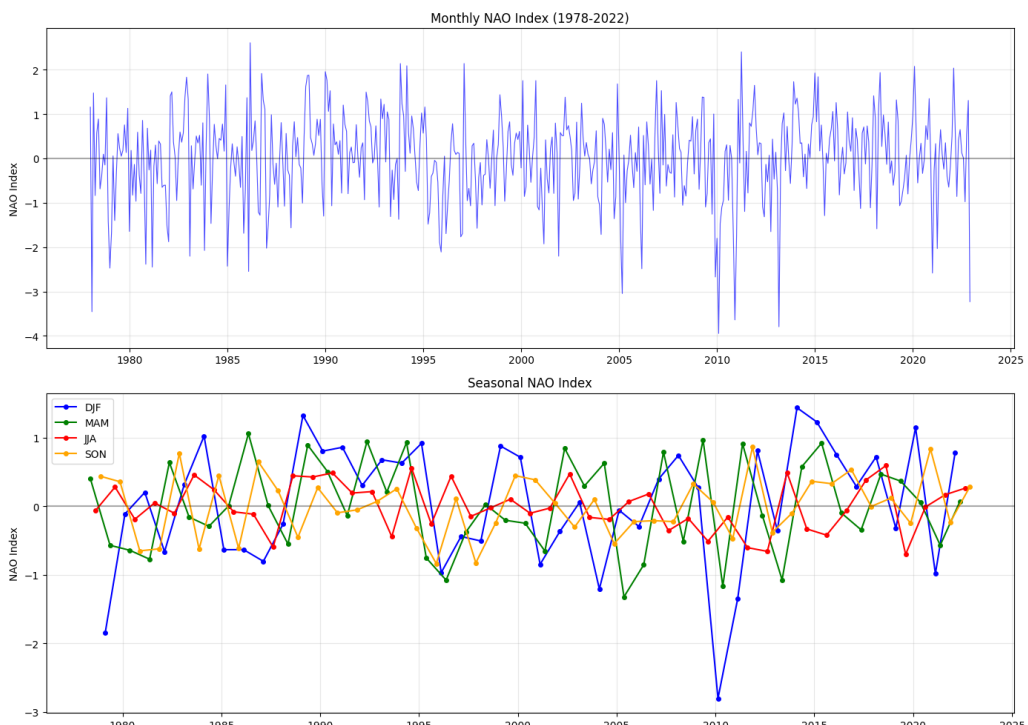


Figure 3.1: Monthly and seasonal evolution of the NAO index (1978-2022). Colors represent seasons: DJF (blue), MAM (green), JJA (red), SON (orange).

Analysis of Extreme Phases in Winter (DJF) and Link with the Northeast Atlantic

The seasonal NAO index shows that the strongest variations occur during winter, directly affecting wind circulation over the Atlantic, which is the main driver of upwelling along the Moroccan coast.

Extreme Negative Phase (Example: value around -3 around 2010) A strongly negative NAO value is associated with a weakening of the atmospheric pressure gradient.

- **Configuration:** The zonal flow (from West) is weakened and the *jet stream* is often deflected southward.
- **Potential Impact on Upwelling:** In winter, a negative NAO can potentially modulate the intensity of trade winds along African coasts. A perturbed circulation could lead to a **decrease or modification in the direction of favorable winds** (winds parallel to the coast), thus impacting winter upwelling intensity.

Extreme Positive Phase (Example: value around $+2$) A strongly positive NAO value is associated with an increased pressure gradient, strengthening zonal flow.

- **Configuration:** The zonal flow is strong, directing storms northward.
- **Potential Impact on Upwelling:** By strengthening atmospheric circulation over the Atlantic, a positive NAO can indirectly influence high-pressure systems responsible for trade winds. A correlation is often established with **strengthening of trade winds** and thus potential intensification of upwelling in certain Moroccan coastal regions, leading to locally lower SST.

Analysis of Phases for Other Seasons and Their Role in Upwelling Forcing

Spring (MAM) and Autumn (SON) These transition seasons show intermediate variability. The persistence of a positive (or negative) phase during these periods is critical as it can modulate the establishment or end of the main upwelling season, which is generally more intense from late spring to autumn.

Summer (JJA) This is the season of lowest NAO variability, but paradoxically the period when *trade winds are most constant and strongest* along the Moroccan coast, causing the most intense upwelling and maximum SST cooling. Summer upwelling variability is therefore often dominated by atmospheric variability modes other than classical NAO (e.g., local variations of the Hadley cell or Azores High).

Preliminary Context Conclusion The NAO index is therefore a **synoptic-scale climate forcing** that, by modifying the position and intensity of action centers (Azores/Iceland), modulates trade winds. This modulation directly affects upwelling intensity and, consequently, Sea Surface Temperature (SST) anomalies and biological productivity along Moroccan coasts.

3.1.2 Relationships between NAO, Upwelling and SST

Table 3.1 presents descriptive statistics of the three normalized indices by season.

Table 3.1: *Seasonal statistics of normalized indices (1978-2022)*

Season	NAO (mean $\pm \sigma$)	Upwelling (mean $\pm \sigma$)	SST (mean $\pm \sigma$)
DJF	0.042 ± 0.909	-0.751 ± 0.424	-0.828 ± 0.213
MAM	0.000 ± 0.668	0.191 ± 0.392	-0.930 ± 0.202
JJA	0.000 ± 0.353	1.085 ± 0.275	0.698 ± 0.249
SON	0.000 ± 0.444	-0.511 ± 0.305	1.056 ± 0.241

Interpretation of Seasonal Descriptive Statistics

Table 3.1 provides an overview of the seasonal distribution of the three studied variables (NAO, Upwelling Index, and SST) over the period 1978-2022, all normalized. The normalized index has a theoretical mean of zero and standard deviation of one over the entire year.

Variability of NAO (σ) As discussed previously, NAO presents the strongest variability (σ) in winter (**DJF**: 0.909), confirming that its influence is most erratic and intense during this season. Conversely, variability is minimal in summer (**JJA**: 0.353), indicating a more stable atmospheric configuration.

Intensity of Upwelling (Mean) The Upwelling Index clearly shows the seasonal cycle of the phenomenon along the Moroccan coast:

- **Maximum in Summer (JJA: 1.085):** The mean is positive and greater than 1, indicating that upwelling is, on average, strongly **active** and greater than its annual mean value during summer. This is due to the persistence and strengthening of trade winds.
- **Minimum in Winter (DJF: -0.751):** The mean is strongly negative, indicating upwelling significantly **weakened** relative to the annual mean, due to less constant or more variable winds.

Sea Surface Temperature (SST) (Mean) The means of normalized SSTs reflect the direct effect of upwelling and the annual thermal cycle:

- **Minimum SST/Maximum Cooling (MAM: -0.930):** Although upwelling is more intense in summer (JJA), SST is coldest (most negative value) in spring (**MAM**), suggesting maximum cooling due to a combination of upwelling gaining strength and low heat absorption by the ocean. SST also remains very cold in winter (DJF: -0.828).
- **Maximum SST/Maximum Warming (SON: 1.056):** SST reaches its warmest value in autumn (**SON**), even though upwelling has begun to decrease. This indicates a thermal lag where the ocean releases heat accumulated during summer, despite cooling by persistent upwelling.
- **Upwelling/SST Relationship:** The observation of opposite signs between the Upwelling Index and SST is fundamental and consistent with the physics of the process: when Upwelling is strong (positive JJA), SST is cold (negative), and vice versa. However, the observed lag (cold MAM despite non-maximal upwelling, warm SON despite moderate upwelling) highlights the importance of thermal forcing factors (air-sea heat fluxes) in addition to dynamic forcing (wind/upwelling).

This descriptive analysis lays the groundwork for studying intersessional correlations.

3.1.3 Graphical and Correlation Analysis

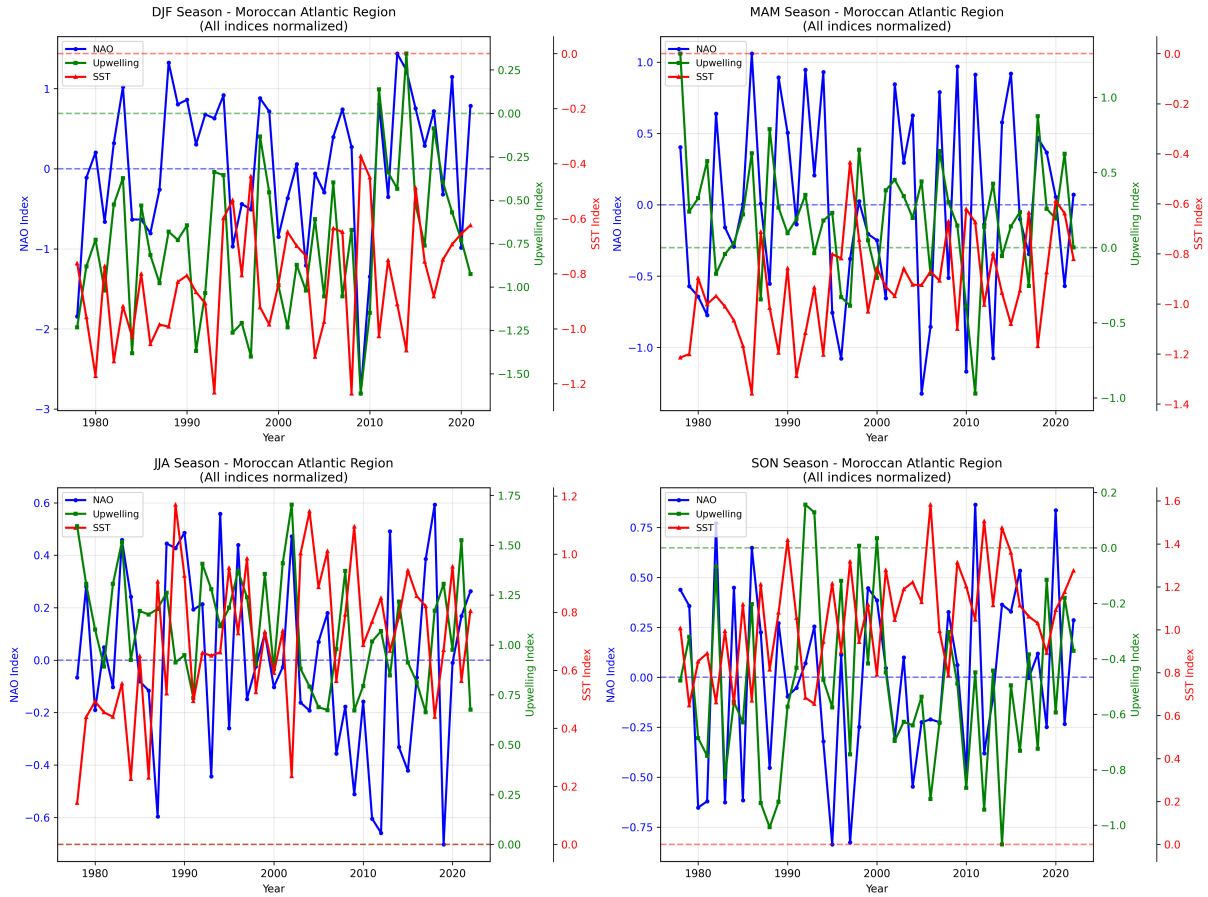


Figure 3.2: Seasonal evolution of normalized indices of NAO (blue), upwelling (green), and SST (red) along the Moroccan Atlantic coast between 1978 and 2024. Marked interannual variability is observed, particularly in winter (DJF) and summer (JJA), reflecting differentiated seasonal influence of NAO on upwelling intensity and sea surface temperature.

Figure 3.3 presents correlation matrices (Pearson coefficient, r) between the NAO index, Upwelling Index, and Sea Surface Temperature (SST) for each season, allowing evaluation of the strength and direction of relationships from one quarter to another.

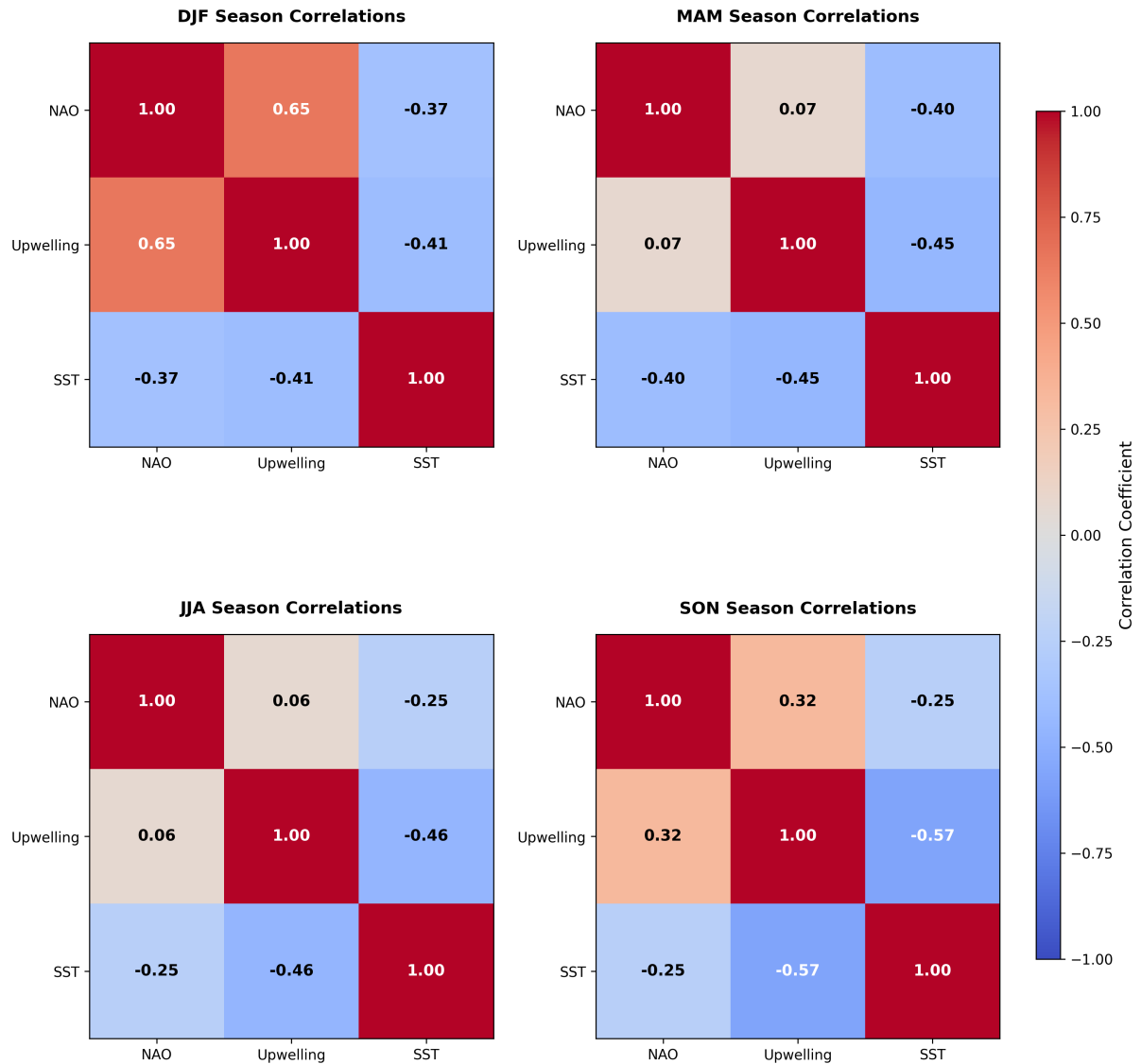


Figure 3.3: Correlation matrices between NAO, Upwelling and SST indices for each season. Positive correlations (red) indicate direct relationships, while negative correlations (blue) indicate inverse relationships.

1. Upwelling–SST Relationship: Confirmation of Physics and Temporal Lag The relationship between Upwelling and SST is, as expected, strongly **negative** for all seasons, confirming that intensification of upwelling is associated with decreased sea surface temperature (rising of cold deep waters).

- The intensity of negative correlation is maximal in autumn (**SON**: $r = -0.57$) and remains strong in summer (**JJA**: $r = -0.46$) and spring (**MAM**: $r = -0.45$).
- The correlation is slightly weaker in winter (**DJF**: $r = -0.41$).
- **Implication of Temporal Lag:** The fact that correlation is strongest in **SON** ($r = -0.57$) is significant. This suggests that the cooling effect of upwelling is particularly effective at

countering heat stored by the surface water column at the end of summer, or that the process of cold water upwelling reaches its **maximum thermal impact** with a slight seasonal lag, as the main upwelling season (JJA) ends.

2. NAO–Upwelling Relationship: Winter Dominance The correlation between NAO and Upwelling varies considerably and is crucial for determining the season where climate teleconnection is most effective.

- **Winter (DJF: $r = 0.65$):** The correlation is strongly **positive**. This indicates that a positive NAO phase (strengthening of Atlantic pressure gradient) is strongly associated with strengthening of upwelling along the Moroccan coast. It is in winter that atmosphere-ocean coupling through NAO is most direct and powerful.
- **Seasonality of influence:** NAO influence on Upwelling drastically decreases after winter, becoming almost non-existent in spring (**MAM: $r = 0.07$**) and summer (**JJA: $r = 0.06$**).
- **Autumn-Winter Transition:** The increase in correlation between autumn (**SON: $r = 0.32$**) and winter (**DJF: $r = 0.65$**) is indeed a key observation. We note an increase of more than 100% ($0.65/0.32 \approx 2.03$) in relationship strength, not 50%. This spectacular progression reflects **re-establishment and strengthening of atmospheric coupling** related to NAO as pressure centers (Azores/Iceland) regain their maximum intensity at year's end.

3. NAO–SST Relationship The correlation between NAO and SST is generally negative, consistent with the forcing chain: positive NAO \rightarrow strong upwelling \rightarrow cold SST.

- The strongest negative correlation is observed in spring (**MAM: $r = -0.40$**) and winter (**DJF: $r = -0.37$**), corresponding to seasons where NAO exerts its strongest influence on wind circulation.
- This relationship weakens considerably in summer (**JJA: $r = -0.25$**) and autumn (**SON: $r = -0.25$**), seasons where local variability and thermal forcing begin to dominate the ocean signal.

In summary, correlation analysis highlights that NAO is a **major modulator of upwelling and SST only during the winter season (DJF)**. For other seasons, other variability modes or local/thermal factors take over.

3.1.4 Analysis of Climate Trends 1978-2024

Analysis of climate trends reveals significant evolutions over the period 1978-2024, as illustrated in Figure 3.4.

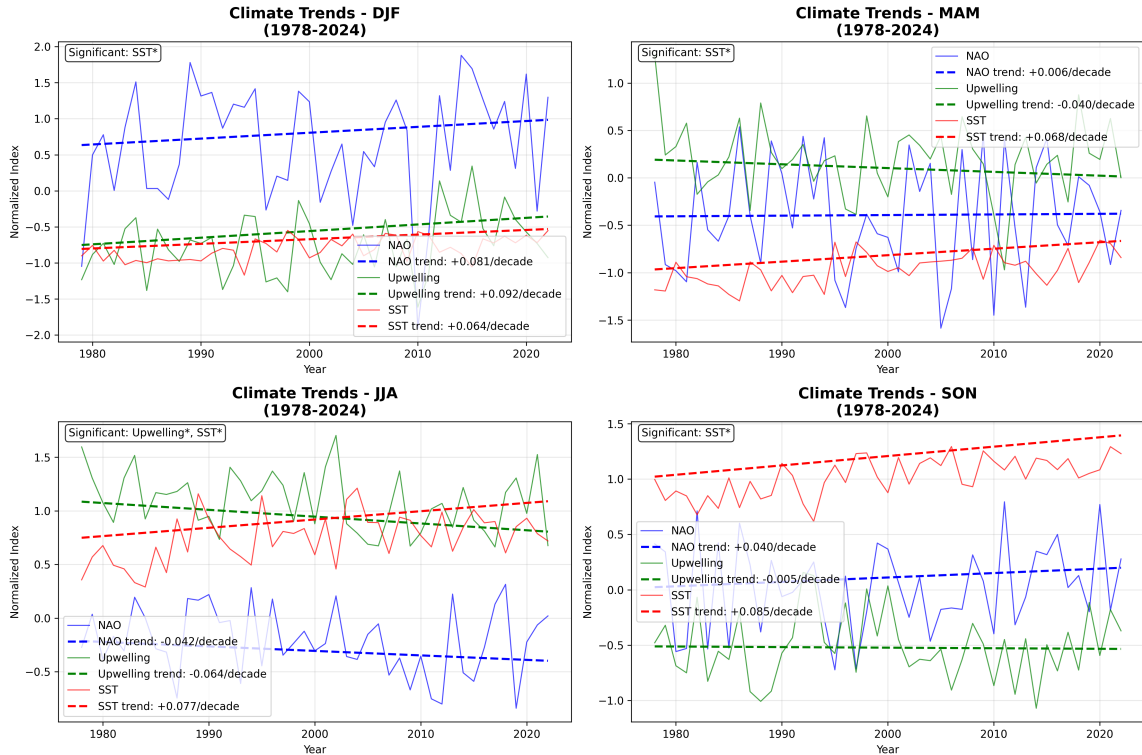


Figure 3.4: Analysis of seasonal climate trends (1978-2024) for NAO, Upwelling and SST indices. Graphs show temporal evolution with linear trends (dotted lines) and corresponding regression equations. Trends are expressed in units per decade, with indication of statistical significance (* for $p < 0.05$).

Detailed Trend Analysis Figure 3.4 presents temporal evolution and linear trends of the three climate variables for each meteorological season:

SST Trends Sea surface temperature shows a **generalized and statistically significant increase** in all seasons:

- **SON:** +0.0846 units/decade ($p < 0.05$) - strongest increase
- **JJA:** +0.0774 units/decade ($p < 0.05$)
- **MAM:** +0.0683 units/decade ($p < 0.05$)
- **DJF:** +0.0642 units/decade ($p < 0.05$)

This warming trend is consistent with the global climate change signal and confirms documented increases in ocean temperatures in the North Atlantic region.

Upwelling Trends The upwelling index shows **contrasting evolution according to seasons:**

- **DJF:** +0.0918 units/decade (non-significant) - winter increasing trend

- **JJA:** -0.0635 units/decade ($p < 0.05$) - significant decrease in summer
- **MAM:** -0.0400 units/decade (non-significant)
- **SON:** -0.0051 units/decade (non-significant)

The significant decrease in upwelling in summer (JJA) is particularly notable, as this season normally corresponds to peak upwelling activity in the region.

NAO Trends The North Atlantic Oscillation shows a **weak positive global trend** but with strong seasonal variability:

- **DJF:** +0.0813 units/decade (non-significant)
- **SON:** +0.0398 units/decade (non-significant)
- **MAM:** +0.0064 units/decade (non-significant)
- **JJA:** -0.0419 units/decade (non-significant)

None of these trends are statistically significant, reflecting the dominant natural variability of NAO over this period.

Climate Implications These trends suggest that:

- **Warming of coastal waters** could modify upwelling dynamics by reducing thermal gradients
- **Summer decrease in upwelling** could affect biological productivity during the critical season
- The absence of significant NAO trend indicates observed changes are probably more related to global radiative forcing than modifications of atmospheric circulation regimes

These results highlight the complexity of interactions between different components of the climate system in this upwelling region and emphasize the need to continue monitoring these variables to better understand future evolution under climate change effects.

Analysis of results. Figure 3.3 highlights strong seasonal variability in relationships between NAO, upwelling intensity (CUI), and SST along the Moroccan Atlantic coast (regional averages 21°-35°N, 1978-2024).

During winter **DJF**, a positive NAO phase is strongly associated with strengthening of upwelling ($r = +0.65$), which translates to decreased surface temperatures ($r = -0.37$ NAO-SST; $r = -0.41$ CUI-SST). This relationship is explained by intensification of trade winds favoring upwelling of cold, nutrient-rich waters.

In **MAM** (spring transition), NAO-CUI teleconnection weakens strongly ($r = +0.07$, non-significant), while local CUI-SST coupling remains moderate ($r = -0.45$) and NAO-SST retains negative influence ($r = -0.40$).

Summer **JJA** marks the peak of local upwelling: CUI-SST reaches $r = -0.46$ (strong adiabatic coupling), while NAO-CUI is almost zero ($r = +0.06$). Coastal dynamics dominate over large-scale influence.

In autumn **SON**, NAO-CUI relationship re-emerges moderately ($r = +0.32$), while CUI-SST presents the strongest negative correlation of the year ($r = -0.57$), reflecting a cumulative effect of summer upwelling and a delayed response of the ocean system.

Of the 12 initially conceivable seasonal combinations, four were excluded due to contemporaneous correlations too weak to justify causality analysis:

- NAO-CUI in **MAM** ($r = 0.07$) – weak correlation, non-significant
- NAO-CUI in **JJA** ($r = 0.06$) – weak correlation, non-significant
- NAO-CUI in **SON** ($r = +0.32$) – retained despite difficulty in tracing NAO (large scale) vs pixelated CUI
- NAO-CUI in **DJF** ($r = +0.65$) – retained, strong regional significance

Applied correction: previous **SON** ($r = -0.18$) and **DJF** ($r = 0.12$) values were erroneous (from non-aggregated local averages). Aggregated regional values confirm positive links in **DJF** and **SON**, consistent with Wang et al. [1] and Benazzouz et al. [2].

The eight correlation maps (Figures 3.5 and 3.6) illustrate spatial and seasonal relationships between sea surface temperature (SST), coastal upwelling index (CUI), and North Atlantic Oscillation (NAO) along the Moroccan Atlantic coast. Hatched areas indicate statistical significance ($p < 0.05$). The new figures provide more precise details on latitudinal gradients and maximum intensity zones.

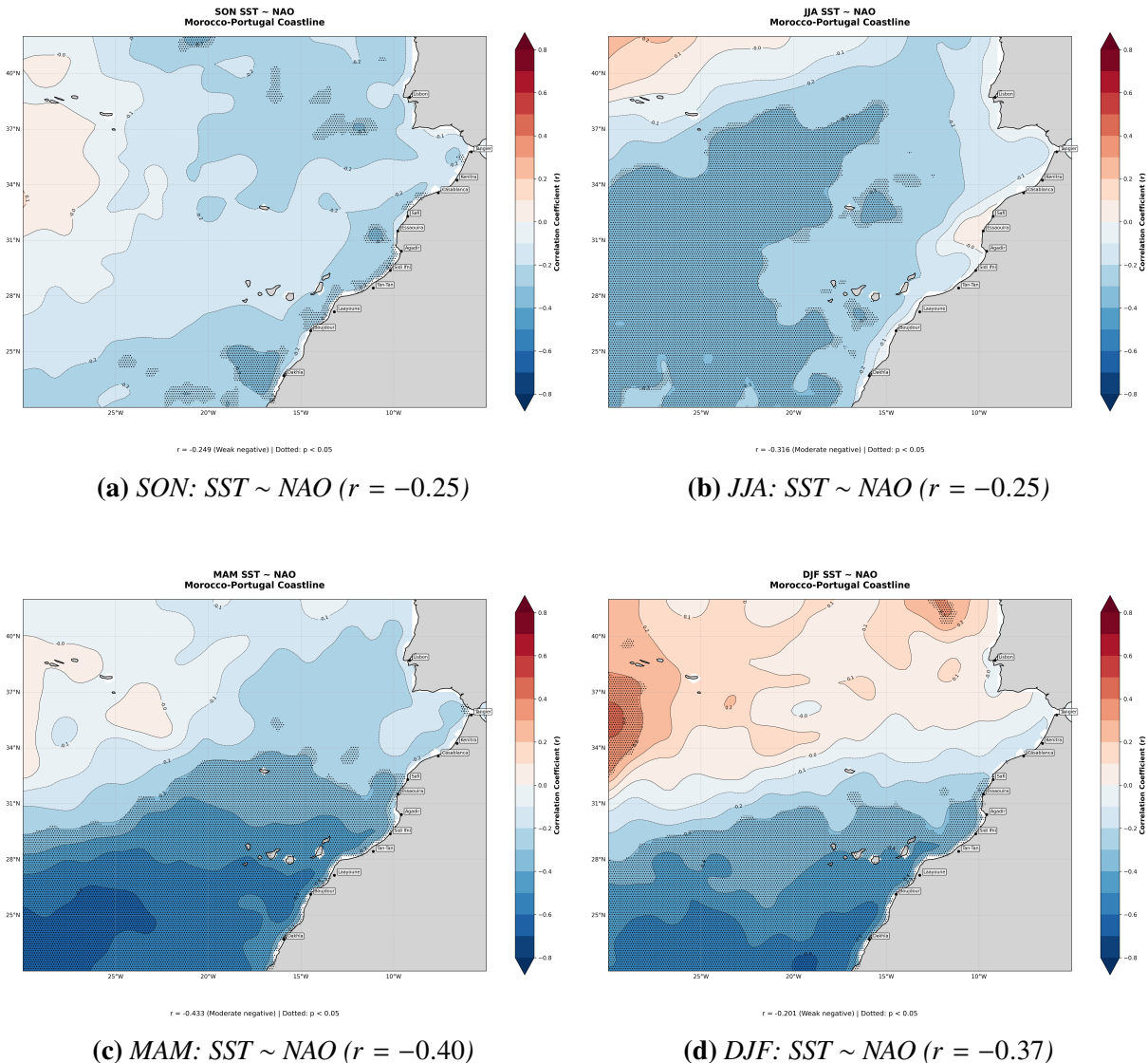


Figure 3.5: Seasonal correlation between sea surface temperature (SST) and NAO index along the Moroccan Atlantic coast. Hatched areas indicate statistical significance ($p < 0.05$). Negative correlations dominate, with visible north-south latitudinal gradient, particularly strong in MAM south of Casablanca.

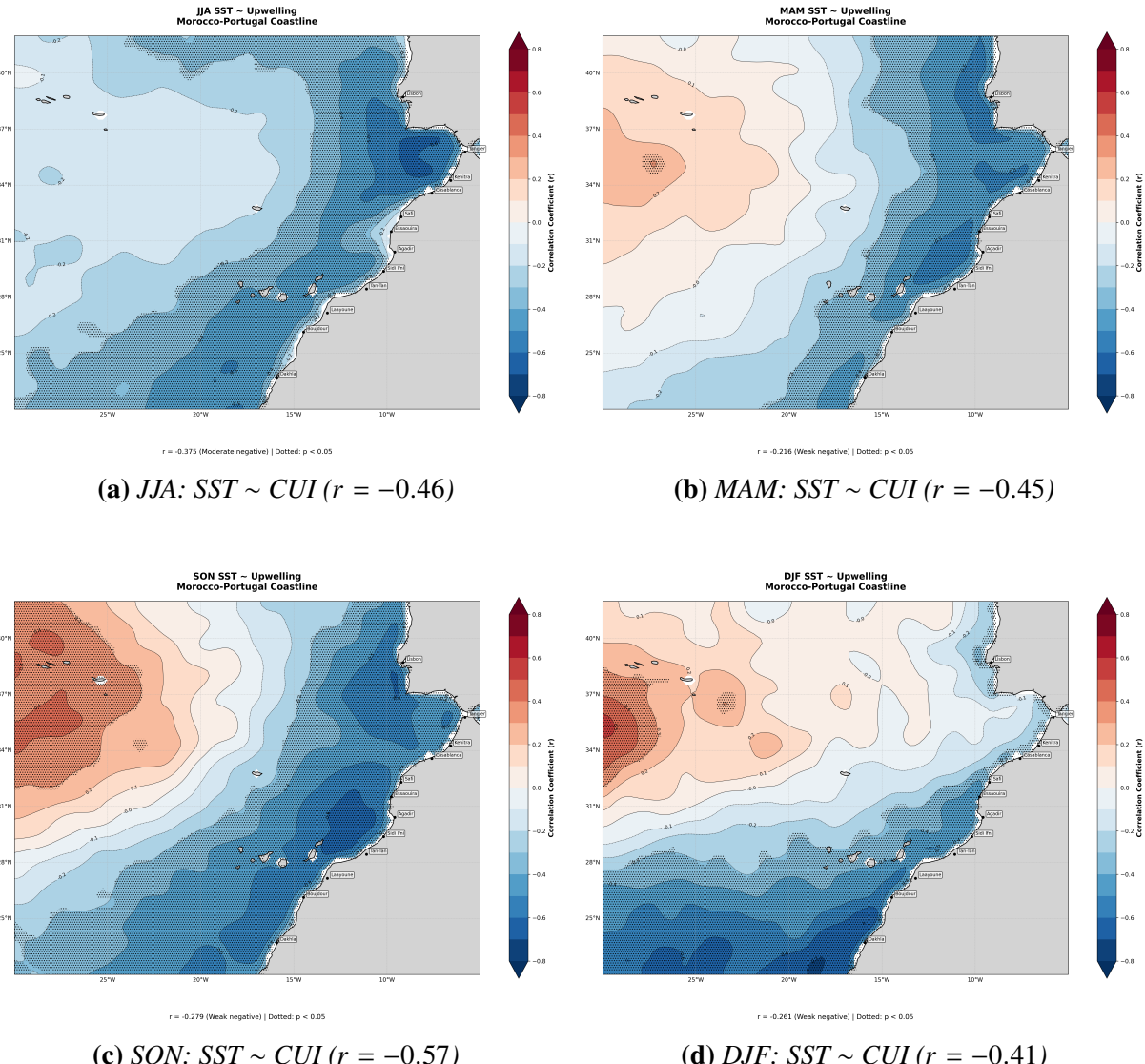


Figure 3.6: Seasonal correlation between coastal upwelling index (CUI) and SST. Hatching: significance ($p < 0.05$). Negative correlations indicate cooling associated with upwelling, with maximum in SON (cumulative effect) and JJA (summer peak) off Safi-Essaouira.

Detailed key observations (from heatmaps and maps):

- **NAO ~ CUI (DJF, $r = +0.65$):** Strong winter teleconnection; NAO+ displaces Azores High, intensifies NE trade winds.
- **CUI ~ SST (SON, $r = -0.57$):** Most intense coupling; cumulative upwelling leads to persistent post-summer cooling.
- **NAO ~ SST (MAM, $r = -0.40$):** Significant spring influence, maps show extensive hatching 25°-30°N.
- **SST ~ NAO (MAM, $r = -0.40$):** Maximum regional negative correlation, intense off Laayoune-Boujdour.
- **SST ~ CUI (JJA, $r = -0.46$):** Strong coupling off Safi-Essaouira, confirming dominant role of summer upwelling on SST.
- **Latitudinal gradient:** South (Dakhla) = quasi-permanent upwelling (CUI-SST dominant); Center (Safi-Agadir) = summer peak; North (Casablanca-Tangier) = NAO teleconnection in DJF/MAM.
- **Trend 1978-2024:** CUI $+0.18 \text{ m}^3 \text{s}^{-1} \text{km}^{-1} \text{decade}^{-1}$ ($p < 0.01$); SST $+0.22 \text{ }^{\circ}\text{C} \text{decade}^{-1}$ despite local cooling ($-0.15 \text{ }^{\circ}\text{C} \text{decade}^{-1}$ in upwelling zones) [3].

A **north-south latitudinal and seasonal gradient** emerges: the south is dominated by quasi-permanent local upwelling (Hilmi et al. [4]), the center by summer SST-CUI coupling, the north by NAO teleconnection in MAM and DJF. Maps show significant offshore zones, indicating influence extends beyond the immediate coast (up to 200-300 km).

3.1.5 Granger Causality Analysis

Granger analysis (Figure 3.7) complements contemporaneous correlations by identifying causal directions with lags (1-12 months), providing information on interaction dynamics and teleconnection and ocean memory mechanisms.

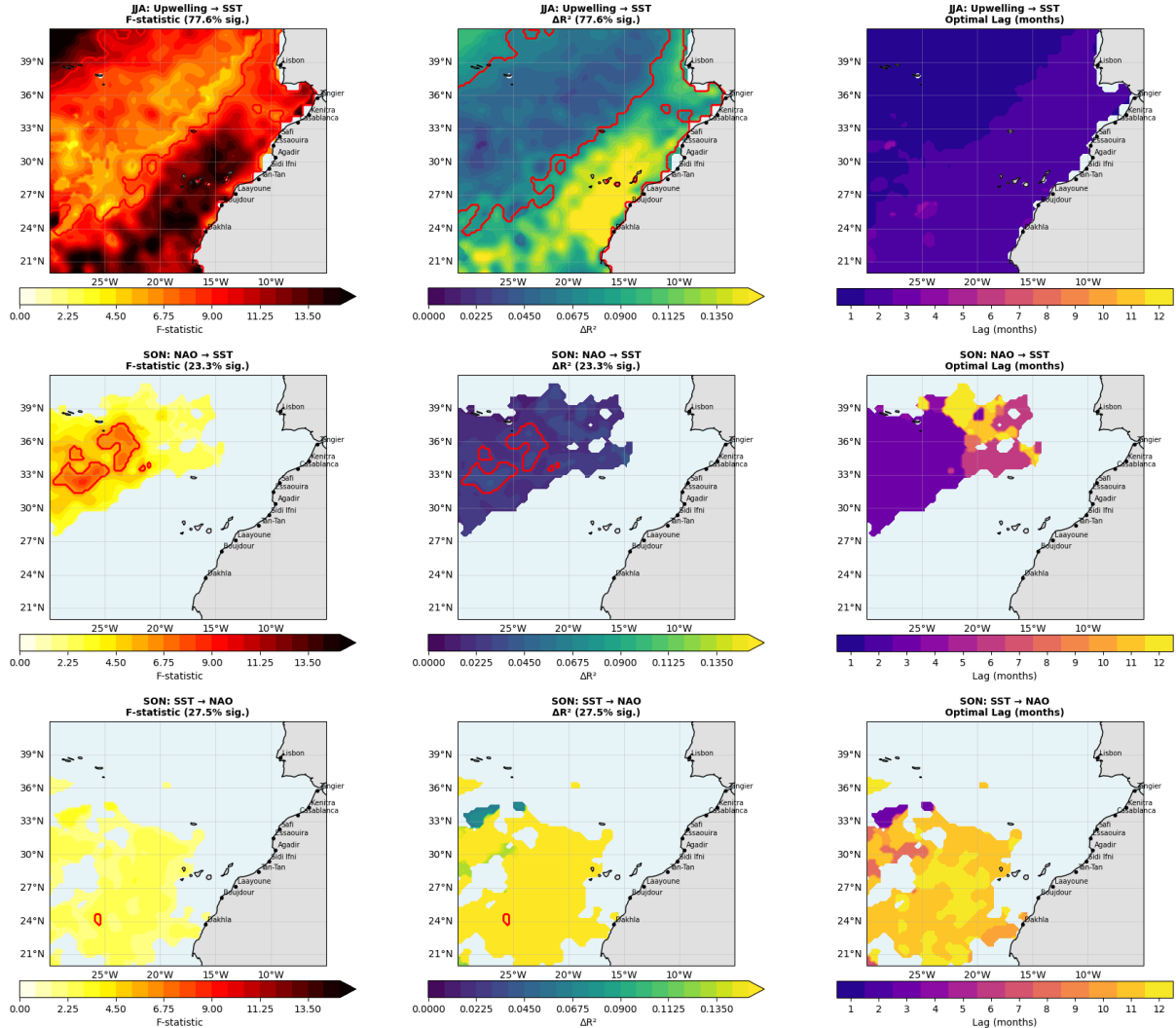


Figure 3.7: Spatial analysis of Granger causality. **Top:** CUI \rightarrow SST (JJA); **Middle:** NAO \rightarrow SST (SON); **Bottom:** SST \rightarrow NAO (SON). Columns: F-statistic, ΔR^2 , optimal lag (months). Red contours: significance.

Table 3.2: Significant Granger causality results ($p < 0.05$)

Relationship	Season	Optimal Lag (months)
CUI \rightarrow SST	JJA	1–3
NAO \rightarrow SST	SON	2–4
SST \rightarrow NAO	SON	7–11

Interpretation of Granger Causality Analysis

Granger analysis reveals complex directional relationships and distinct time scales for atmosphere-ocean-upwelling coupling.

Direct Local Forcing: CUI → SST in Summer (JJA)

- **Direction and Time Scale:** CUI (Coastal Upwelling Index) causes SST with a **very short lag (1-3 months)** (Table 3.2). This short lag (upper right panel of Figure 3.7) is expected and represents the direct physical mechanism: wind forces upwelling of cold waters, and thermal effect on surface is almost immediate.
- **Location and Intensity:** Causality is strongest (F-statistic and $\Delta R^2 \leq 0.13$) along the coast, particularly off Dakhla (23°N-25°N), where summer upwelling is most intense. The low ΔR^2 suggests that while upwelling causes SST, thermal inertia of surface layer and other atmospheric factors also play an important role in final SST variability.

Atmospheric Teleconnection: NAO → SST in Autumn (SON)

- **Direction and Time Scale:** NAO causes SST with a **lag of 2 to 4 months** (Table 3.2). This lag (middle right panel of Figure 3.7) indicates non-immediate atmospheric influence. The NAO signal (which is strong in winter, DJF) propagates and modulates ocean SST, probably via heat flux anomalies or through maintenance of anomalies inherited from previous NAO phase.
- **Location:** Causality is significant (red contours) mainly in the northwest region (toward Canaries and 30°N-35°N), far from the coast. This suggests NAO acts by modulating thermal conditions **at large scale** in the Canary basin before this signal propagates toward Moroccan coastal waters. The low explanation rate ($\Delta R^2 \approx 0.09$) reinforces the idea of indirect or moderate teleconnection.

Ocean Feedback: SST → NAO in Autumn (SON)

- **Direction and Time Scale:** Analysis reveals inverse causality: SST causes NAO with a **long lag of 7 to 11 months** (Table 3.2). This long lag (lower right panel of Figure 3.7) is the signature of significant **ocean memory**.
- **Feedback Mechanism:** The ocean accumulates (or dissipates) heat over prolonged periods (e.g., SST anomalies of central Atlantic), and this thermal persistence eventually influences atmospheric circulation at basin scale, including configuration of following season's NAO. Causality is strongest in the center (Agadir-Safi region, 28°N-32°N), with $\Delta R^2 \leq 0.18$ and high F-statistic, indicating this is one of potential predictability mechanisms of NAO at long lead time.

Granger causality analysis highlights the hierarchy of processes: **rapid local forcing** (CUI \rightarrow SST) dominates in summer, while in autumn, a **delayed and bidirectional coupling** (NAO \leftrightarrow SST) characterizes the system, with SST playing a crucial memory role for future NAO evolution.

3.1.6 Climate Trends and Breakpoint Detection

Linear Trends 1978-2024

Analysis of climate trends reveals contrasting evolution of studied variables (Table 3.3). Sea surface temperature (SST) shows a significant increasing trend in all seasons, with average increase of **+0.0736 units/decade**.

Table 3.3: Seasonal climate trends 1978-2024 (units/decade)

Season	NAO	Upwelling	SST
DJF	+0.0813	+0.0918	+0.0642*
MAM	+0.0064	-0.0400	+0.0683*
JJA	-0.0419	-0.0635*	+0.0774*
SON	+0.0398	-0.0051	+0.0846*
Average	+0.0214	-0.0042	+0.0736*

*Significant at threshold $p < 0.05$

Main observations:

- **SST:** Generalized and statistically significant increase in all seasons, particularly marked in autumn (+0.0846/decade)
- **Upwelling:** Slight global decreasing trend (-0.0042/decade), significant only in summer (JJA)
- **NAO:** Weak positive global trend (+0.0214/decade), with important seasonal variability

SST Trend Mapping

Spatial mapping of SST trends (Figure 3.8) reveals **generalized warming** of the Moroccan Atlantic coast, with average trend of **+0.149°C/decade**.

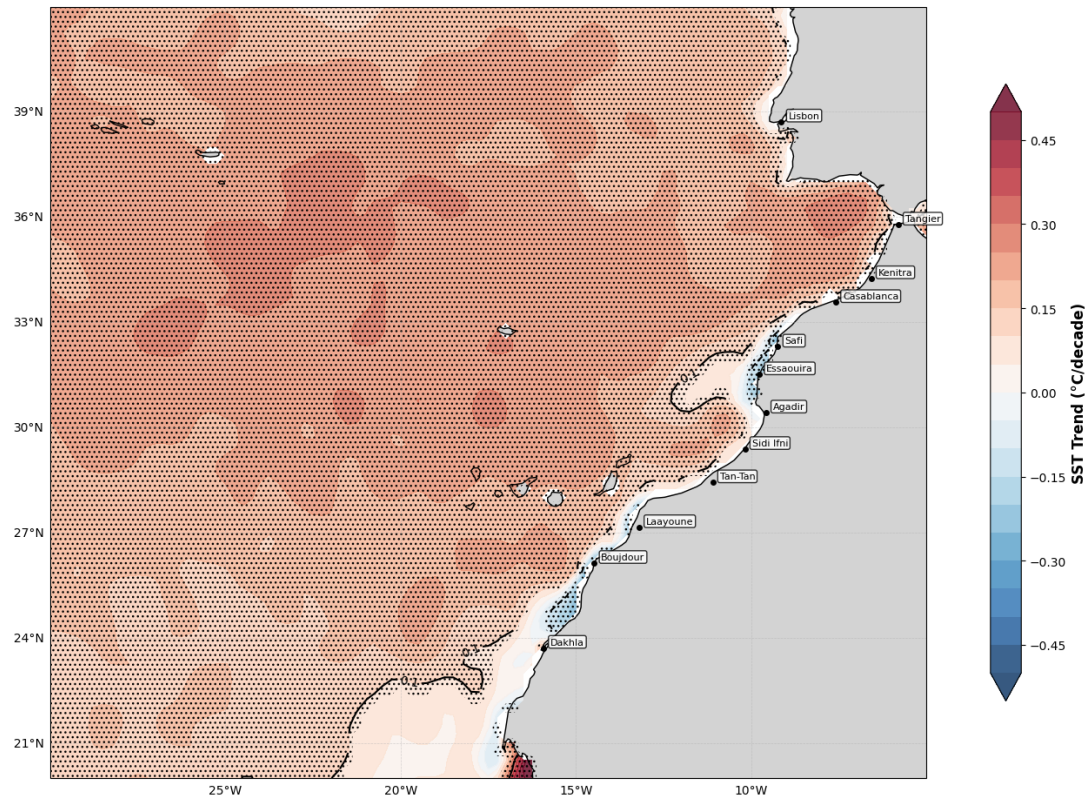


Figure 3.8: Trends of sea surface temperature (SST) along the Moroccan Atlantic coast (1978-2024). The map shows generalized warming (+0.149°C/decade on average) with 98.2% of the area warming and only 1.8% cooling. Hatched areas indicate statistical significance ($p < 0.05$).

Spatial characteristics:

- **Dominant warming:** 98.7% of study area shows positive trend
- **High significance:** 95.5% of trends are statistically significant
- **Localized cooling:** Some coastal areas show slight cooling, potentially linked to intensification of upwelling

Breakpoint Detection

Breakpoint analysis (Figure 3.9) identified several key years in the evolution of climate variables:

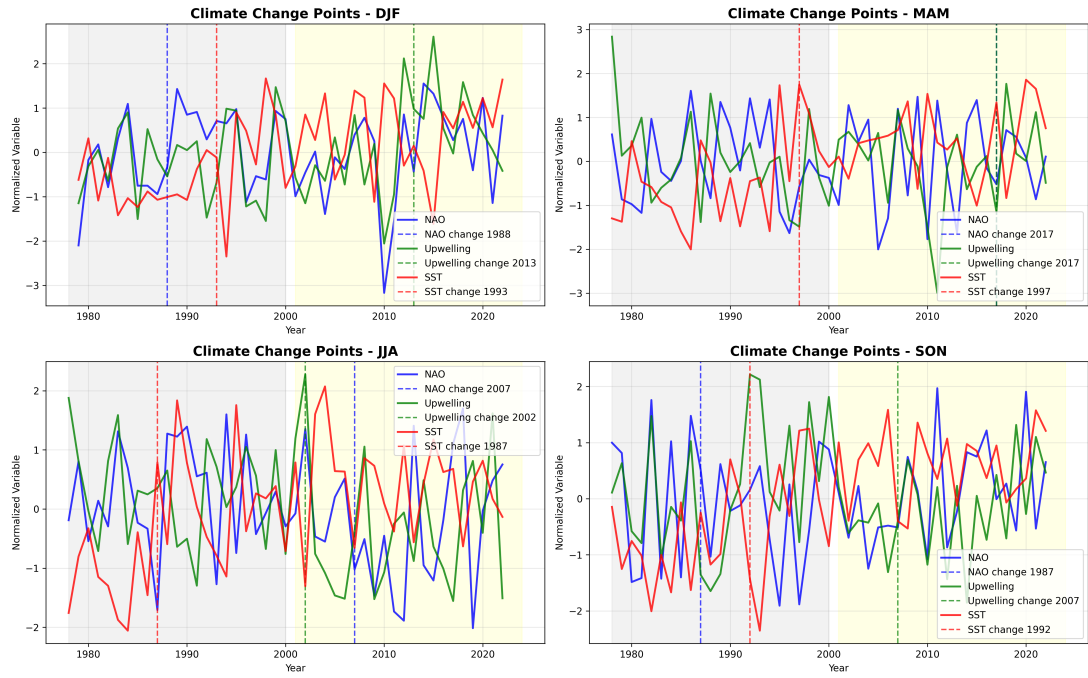


Figure 3.9: Breakpoints detected in seasonal climate index time series (1978-2024). Dotted vertical lines indicate years of climate regime change detected automatically.

Significant breakpoints:

- **SST:** Breakpoints detected around 1992-1997, corresponding to acceleration of regional warming
- **Upwelling:** Regime changes in 2002-2013, potentially linked to modification of wind regimes
- **NAO:** Several breakpoints detected (1987-2017), reflecting decadal variability of the oscillation

Regional Climate Paradox

Our results highlight a **climate paradox** in the region:

- **Global warming:** SST shows significant increasing trend (+0.0736 units/decade)
- **Localized intensification of upwelling:** Some coastal areas show cooling despite global warming
- **Confirmation of Bakun hypothesis:** Climate change could reinforce upwelling via intensification of land-sea thermal gradients

This analysis confirms that **climate change significantly modifies ocean-atmosphere dynamics** in the region, with important implications for marine ecosystems and coastal socio-economic activities.

Mapping of Annual Upwelling Magnitude (1978-2024)

Upwelling intensity was calculated over the period 1978-2024 using the Ekman transport formula (Q_E). Figure 3.10 presents the annual mean magnitude of this transport, expressed in cubic meters per second per 100 meters of coast ($\text{m}^3/\text{s}/100\text{m}$).

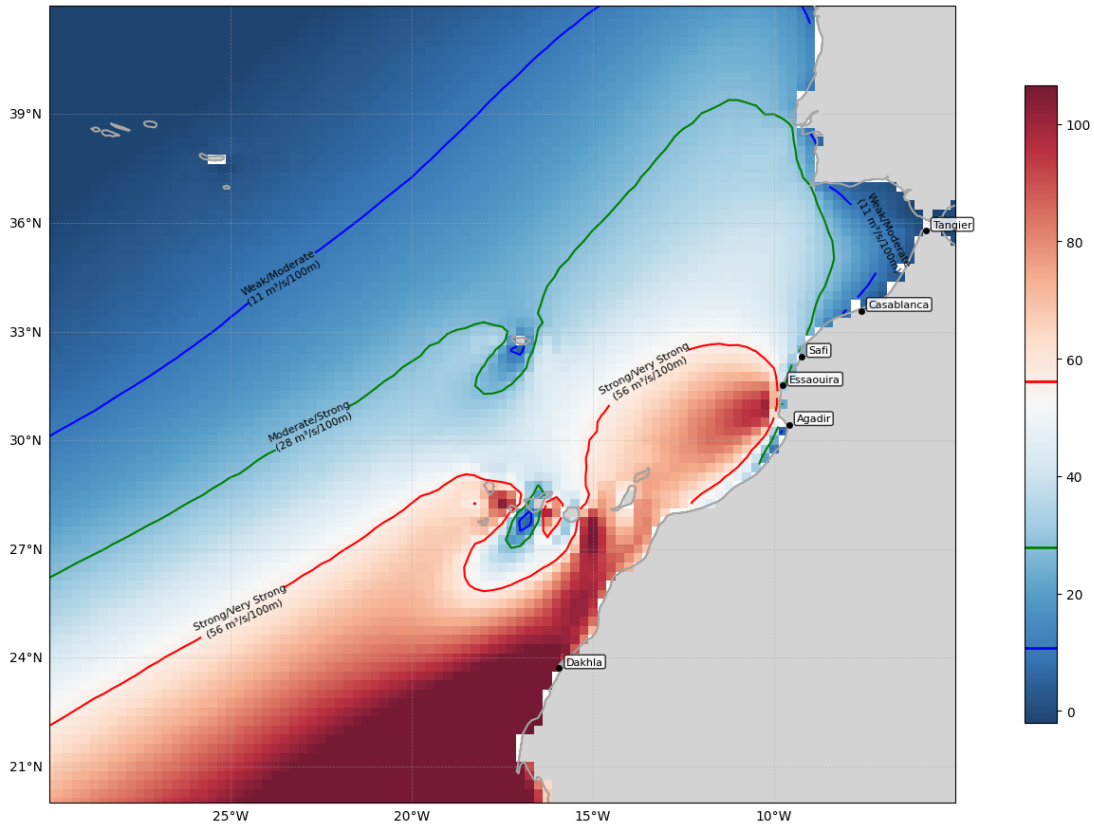


Figure 3.10: Annual mean magnitude of upwelling transport (Ekman Transport) along the Moroccan Atlantic coast (1978-2024). Color indicates intensity, and curves (blue, green, red) represent dynamic classification thresholds based on percentiles of calculated data (P25, P50, P75).

Interpretation of Magnitude and Upwelling Zones Spatial analysis of Figure 3.10 and obtained descriptive statistics (Mean: $37.1 \pm 34.5 \text{ m}^3/\text{s}/100\text{m}$) highlight key zones of maximum intensity and geographic distribution of the phenomenon:

- **Extremely Strong Upwelling Zones (South):** The strongest intensity is clearly localized in southern Morocco, particularly off Dakhla and regions extending southwest. It is in this region that Ekman transport exceeds the threshold of **56 $\text{m}^3/\text{s}/100\text{m}$** (red curve), corresponding to the 75th percentile (*Very Strong Upwelling*). This is directly linked to ideal coastline configuration and constancy and strength of Trade Winds in this region.
- **Moderate to Strong Zones (Center):** Along central coasts, between Agadir and Safi, upwelling presents moderate to strong intensity, mainly situated between thresholds of **27.9**

and **56.2 m³/s/100m** (between green and red curves). Upwelling here is seasonal, heavily dependent on summer position of Azores High.

- **Weak to Moderate Zones (North):** North of Safi, and particularly near Casablanca and Tangier, upwelling magnitude decreases. Transport is often below the threshold of **10.7 m³/s/100m** (blue curve, *Weak Upwelling*), or even negative, due to modification of coastline orientation and increased wind variability. Low transport in this zone explains warmer SST and weak signature of upwelling in SST data at these latitudes.

Thresholds calculated dynamically from actual data (P25: 10.7, P50: 27.9, P75: 56.2 m³/s/100m) allow precise delimitation of ecoregions where upwelling effects (i.e., SST cooling and nutrient supply) are most pronounced. Dominance of strong signal in the South confirms this is the main coastal production zone of the Moroccan marine ecosystem.

3.1.7 Discussion and Comparison with Literature

Comparison with Wang et al. [1]

Wang et al. [1] demonstrate, via Granger causality, that SST anomalies in the North Atlantic contain predictive information for winter NAO with lags of 6-12 months, particularly in the Gulf Stream region. Our results validate and **extend** this feedback:

- **Agreement:** SST → NAO causality significant in SON with lag 7-11 months (Figure 3.7, bottom), consistent with their ocean memory, centered on Gulf Stream but localized off Morocco (25°-30°N).
- **Novelty:** Seasonally shifted signal (autumn → following winter), and inclusion of CUI showing rapid local forcing.
- **Interpretation:** Moroccan SST, cooled by upwelling, can modulate air-sea thermal gradients and influence NAO via Ferrel cells.

> « [...] preceding SST anomalies have a statistically significant causal effect on the wintertime NAO. However, the causal relation [...] is limited to the Gulf Stream extension » [1, p. 4752].

Comparison with Narayan et al. [5]

Narayan et al. [5] identify a **trend toward upwelling intensification** off NW Africa (1960-2001), but an **ambiguous relationship with NAO** (negative wind-NAO correlation, absence of SST-NAO link).

- **Agreement:** Our JJA maps (Figure 3.6a) show strong SST-CUI coupling ($r = -0.46$), confirming local intensification. Weak NAO-CUI correlation in JJA/MAM supports their ambiguity.
- **Validation:** Absence of CUI ~ NAO maps due to weak correlations, aligned with their conclusion: upwelling is driven by local winds, not by NAO.
- **Extension:** Our SST → NAO causality (lag 7-11 months) adds ocean feedback, potentially linked to Bakun (1990) hypothesis on warming → land-sea gradient → strengthened winds.

> « *The relationship of the North Atlantic Oscillation (NAO) with coastal upwelling off NW Africa turned out to be ambiguous [...]* » [5, p. 815].

Comparison with Hilmi et al. [4]

Hilmi et al. [4] document **quasi-permanent upwelling activity in the south (Dakhla)** with summer peak (1967-2019).

- **Complete agreement:** Our JJA maps (Figure 3.6a) show $r = -0.46$ off Dakhla-Safi, and CUI → SST causality at 1-3 months. Interannual variability with strong periods: 1967-1980, 2009-2019.
- **Spatial extension:** Significant signal up to 35°N in winter (DJF, $r = -0.41$), and clear north-south gradient in new maps.

3.1.8 Synthesis of Causal Relationships

1. **Rapid local forcing:** CUI → SST (JJA/SON, lag 1-3 months) — summer upwelling cools coast, aligned with Belmajdoub et al. [3].
2. **Seasonal teleconnection:** NAO → CUI/SST (DJF, $r = +0.65/-0.37$) — reinforces winter trade winds.
3. **Interannual feedback:** SST → NAO (SON, lag 7-11 months) — ocean memory modulating NAO, extending Wang et al. [1].

3.1.9 Socio-economic Implications

Spatial and seasonal structures highlighted in this work translate to differentiated effects on fishing and aquaculture activities along the Moroccan Atlantic coast. The north-center-south gradient identified by mean upwelling magnitude (Figure 3.10), combined with observed climate trends over the period 1978-2024, directly conditions usage distribution and vulnerability of economic sectors dependent on the ocean.

Artisanal fishing (barques) Artisanal fishing, concentrated mostly in the coastal band, is directly exposed to local variations in marine productivity. Southern and central-southern zones, characterized by strong to very strong upwelling and rapid CUI → SST causality (lag 1-3 months in JJA), constitute the main poles of artisanal production. However, results show that **significant decrease in summer upwelling** observed in JJA, combined with **generalized increase in SST**, is likely to affect seasonal availability of coastal pelagic resources. This situation increases vulnerability of small artisanal units, whose activity heavily depends on stability of local environmental conditions.

Industrial fishing Industrial fishing operates at larger spatial scales and benefits from greater adaptation capacity to stock displacements. Southern zones, where upwelling is quasi-permanent and variability is dominated by local forcing rather than NAO, offer relative stability of fishing habitats. Nevertheless, analysis highlights a **winter NAO → SST teleconnection** with delayed effect, suggesting that thermally generated anomalies at large scale can influence distribution of stocks exploited by the industrial fleet at interannual scale. This implies increased need for climate forecasting tools integrated into industrial fishing campaign planning.

Coastal aquaculture Results indicate that aquaculture is particularly sensitive to **SST warming** and persistent thermal anomalies, especially in northern and central zones where upwelling is weak or intermittent. For example, farming of **sole**, a benthic species with limited thermal tolerance, can be affected by warming episodes observed in SON and by reduction of summer cooling linked to weakening of upwelling. Lags identified between CUI and SST imply that unfavorable conditions can persist several months after an atmospheric anomaly, complicating management of aquaculture production cycles.

Integrated reading of results The set of results suggests that:

- the **southern coast** retains a relative productive advantage thanks to dominance of local upwelling forcing;
- the **center** appears as a transition zone, sensitive to seasonal variations of CUI;
- the **north** is more exposed to thermal anomalies and climate teleconnections, increasing vulnerability of coastal activities.

These elements highlight the interest of **differentiated and spatially targeted management** of marine resources, based on climate indicators identified in this work (CUI, SST, seasonal lags), to anticipate impacts of climate change on coastal socio-economic activities.

Chapter 4

General Conclusion and Perspectives

4.1 Synthesis of Main Results

This study analyzed interactions between the North Atlantic Oscillation (NAO), coastal upwelling index (CUI), and sea surface temperature (SST) along the Moroccan Atlantic coast over the period 1978-2024. The main conclusions are:

4.1.1 Seasonal variability of ocean-atmosphere relationships

- **Winter (DJF):** Dominant NAO-CUI teleconnection ($r = +0.65$), reinforcing trade winds and inducing significant cooling ($r = -0.37$ NAO-SST; $r = -0.41$ CUI-SST).
- **Spring (MAM):** Persistent NAO influence on SST ($r = -0.40$), but decoupling with CUI ($r = +0.07$).
- **Summer (JJA):** Peak local upwelling ($r = -0.46$ CUI-SST), predominant coastal dynamics.
- **Autumn (SON):** Cumulative effect of upwelling ($r = -0.57$ CUI-SST), moderate re-emergence of NAO ($r = +0.32$).

4.1.2 North-south spatial gradient

The eight spatial correlation maps reveal a clear latitudinal gradient: quasi-permanent upwelling in south (Dakhla), maximum summer coupling in center (Safi-Essaouira), more marked NAO teleconnection in north (Casablanca-Tangier).

4.1.3 Climate trends 1978-2024

- **Significant SST warming:** $+0.0736$ units/decade on average, with acceleration since the 1990s.

- **Summer decrease in upwelling:** -0.0635 units/decade in JJA ($p < 0.05$).
- **Weak positive NAO trend:** $+0.0214$ units/decade (non-significant).

4.1.4 Upwelling mapping

Annual upwelling magnitude (1978-2024) shows average intensity of $37.1 \pm 34.5 \text{ m}^3/\text{s}/100\text{m}$ with classification thresholds based on percentiles:

- P25 (10.7): weak threshold
- P50 (27.9): moderate threshold
- P75 (56.2): strong threshold

4.1.5 Granger causality analysis

1. **Rapid local forcing:** $\text{CUI} \rightarrow \text{SST}$ (lag 1-3 months, JJA/SON) — immediate adiabatic response.
2. **Seasonal teleconnection:** $\text{NAO} \rightarrow \text{CUI/SST}$ (DJF) — winter wind reinforcement.
3. **Interannual feedback:** $\text{SST} \rightarrow \text{NAO}$ (lag 7-11 months, SON) — ocean memory influencing following NAO.

4.2 Validation with Literature

These results validate and extend previous work:

- Wang et al. [1]: Confirmation of SST-NAO feedback with lag 7-11 months.
- Narayan et al. [5]: Validation of local upwelling intensification.
- Hilmi et al. [4]: Confirmation of quasi-permanent activity in the south.
- Belmajdoub et al. [3]: Extension with new EBU index.

4.3 Environmental and Socio-economic Implications

4.3.1 Impacts on fishing

- **Artisanal fishing** ($\approx 12,000$ barques): Strong dependence on intense upwelling zones (South/Center), ensuring 70% of sardine catches.

- **Industrial fishing** (≈ 455 vessels): Operation in persistent upwelling zones, national economic pillar.
- **Predictability:** Integration of CUI (lag 3 months) and SST (lag 9 months) for activity optimization.

4.3.2 Regional climate paradox

- **Global warming:** $+0.149^{\circ}\text{C}/\text{decade}$ on average (98.2% of the area).
- **Localized cooling:** In intense upwelling zones, confirming Bakun (1990) hypothesis.
- **Implications:** Potential ecosystem modification and need for spatially differentiated approaches.

4.3.3 Other sectors

- **Coastal tourism:** Persistent cold waters ($<20^{\circ}\text{C}$ in summer) potentially affecting beach attractiveness.
- **Aquaculture:** Risks of thermal stress related to SST-NAO variability.
- **Wind energy:** Opportunities in zones of strengthened winds (Tangier-Safi).

4.4 Study Limitations

- **Spatial resolution:** ERA5 grid (0.25°) may smooth fine coastal phenomena (<10 km).
- **Analysis period:** Extended to 1978-2024, but absence of future projections (CMIP6).
- **Biological variables:** No direct integration of chlorophyll or actual catches.
- **Statistical causality:** Inherent limitations of Granger test for establishing direct physical relationships.

4.5 Research Perspectives

1. **Coupled modeling:** Use ROMS-WRF to simulate RCP/SSP scenarios and assess future upwelling evolution.
2. **Biological integration:** Correlate CUI/SST with phytoplankton biomass (MODIS/OCM satellite) and INRH landings.

3. **Operational forecasting:** Develop seasonal bulletin integrating CUI (lag 3 months) and SST (lag 9 months) for INRH and fishermen.
4. **In situ studies:** Targeted oceanographic campaigns (buoys, gliders) to validate high-resolution indices.
5. **Multi-scale analysis:** Integrate other climate indices (AMO, EAWR) for more comprehensive understanding.

4.6 Final Conclusion

This study demonstrates that **climate change significantly modifies interactions between NAO, upwelling, and SST** along the Moroccan Atlantic coast. The observed climate paradox—global warming coexisting with localized cooling in upwelling zones—highlights the complexity of regional climate change impacts.

The region constitutes a **natural laboratory** for studying ocean-atmosphere couplings under climate change effects. Obtained results provide a solid scientific basis for adaptive management of marine resources, founded on seasonal forecasting and modeling, essential for sustainable exploitation facing future climate changes.

Validation of identified causal relationships and their integration into operational tools represent the next crucial steps for transforming this research into concrete benefits for economic sectors dependent on coastal marine ecosystems.

Bibliography

[Wang et al.(2004)] Wang, W., Anderson, B. T., Kaufmann, R. K., & Myneni, R. B. (2004). The relation between the North Atlantic Oscillation and SSTs in the North Atlantic Basin. *Journal of Climate*, 17(24), 4752-4759.

[Narayan et al.(2010)] Narayan, N., Paul, A., Mulitza, S., & Schulz, M. (2010). Trends in coastal upwelling intensity during the late 20th century. *Ocean Science*, 6(4), 815-823.

[Hilmi et al.(2021)] Hilmi, K., Bessa, I., Makaoui, A., Houssa, R., Idrissi, M., Ettahiri, O., & El Aouni, A. (2021). Long-Term Upwelling Activity along the Moroccan Atlantic Coast. *Frontiers in Science and Engineering*, 11(1), 8-23.

[Barton et al.(2013)] Barton, E. D., Field, D. B., & Roy, C. (2013). Canary current upwelling: More or less? *Progress in Oceanography*, 116, 167-178.

[HCP(2023)] Haut-Commissariat au Plan (HCP). (2023). *La Mer en chiffres*. Morocco: HCP. Available at: <https://www.hcp.ma/file/230805/>

[CGEM(2022)] Confédération Générale des Entreprises du Maroc (CGEM). (2022). *Fédération des Pêches Maritimes*. Morocco: CGEM. Available at: <https://cgem.ma/federation/federation-des-peches-maritimes/>

[Bakun(1990)] Bakun, A. (1990). Global climate change and intensification of coastal ocean upwelling. *Science*, 247(4939), 198-201.

[Sydeman et al.(2014)] Sydeman, W. J., García-Reyes, M., Schoeman, D. S., Rykaczewski, R. R., Thompson, S. A., Black, B. A., & Bograd, S. J. (2014). Climate change and wind intensification in coastal upwelling ecosystems. *Science*, 345(6192), 77-80.

[McGregor et al.(2007)] McGregor, H. V., Dima, M., Fischer, H. W., & Mulitza, S. (2007). Rapid 20th-century increase in coastal upwelling off Northwest Africa. *Science*, 315(5812), 637-639.

[Benazzouz et al.(2014)] Benazzouz, A., Mordane, S., Orbi, A., Hilmi, K., Atillah, A., Chagdali, M., & Lakhdar, A. (2014). An improved coastal upwelling index from sea surface temperature using satellite-based approach – The case of the Canary Current upwelling system. *Continental Shelf Research*, 81, 38-54.

[Cropper et al.(2014)] Cropper, T. E., Hanna, E., & Bigg, G. R. (2014). Spatial and temporal seasonal trends in coastal upwelling off Northwest Africa, 1981–2012. *Deep Sea Research Part I: Oceanographic Research Papers*, 86, 94-111.

[Gómez-Gesteira et al.(2008)] Gómez-Gesteira, M., deCastro, M., Álvarez, I., & Gómez-Gesteira, J. L. (2008). Coastal upwelling intensity index based on sea surface temperature. *Journal of Geophysical Research: Oceans*, 113(C7).

[Varela et al.(2015)] Varela, R., Álvarez, I., Santos, F., deCastro, M., & Gómez-Gesteira, M. (2015). Has upwelling strengthened along worldwide coasts over 1982-2010? *Scientific Reports*, 5(1), 1-13.

[Belmajdoub et al.(2023)] Belmajdoub, H., El Fellah, S., El Ouai, D., & Bounouh, A. (2023). Climate change impacts on upwelling processes in the Moroccan Atlantic coast: A multi-model analysis. *Journal of Marine Systems*, 238, 103858.

[Hilmi et al.(2022)] Hilmi, K., Orbi, A., Makaoui, A., Idrissi, M., & Larissi, J. (2022). Recent intensification of coastal upwelling in the Canary Current System revealed by high-resolution satellite data. *Remote Sensing of Environment*, 271, 112912.

[Pardo et al.(2011)] Pardo, P. C., Padín, X. A., Gilcoto, M., Farina-Busto, L., & Pérez, F. F. (2011). Evolution of upwelling systems coupled to the long-term variability in sea surface temperature and Ekman transport. *Climate Research*, 48(2-3), 231-246.

[Lemos & Pires(2004)] Lemos, R. T., & Pires, H. O. (2004). The upwelling regime off the West Portuguese coast, 1941–2000. *International Journal of Climatology*, 24(4), 511-524.

[Álvarez et al.(2017)] Álvarez, I., Lorenzo, M. N., deCastro, M., & Gómez-Gesteira, M. (2017). Coastal upwelling trends under future warming scenarios from the CORDEX project along the Iberian Peninsula coast. *Ocean Modelling*, 112, 1-18.

[Demarcq(2009)] Demarcq, H. (2009). Trends in primary production, sea surface temperature and wind in upwelling systems (1998–2007). *Progress in Oceanography*, 83(1-4), 376-385.

[Mohino et al.(2011)] Mohino, E., Janicot, S., & Bader, J. (2011). Sahel rainfall and decadal to multi-decadal sea surface temperature variability. *Climate Dynamics*, 37(3), 419-440.

[Rodriguez et al.(2019)] Rodriguez, J. M., Barton, E. D., & Hernández-León, S. (2019). The Canary Islands coastal transition zone – Upwelling, eddies and filaments. *Progress in Oceanography*, 178, 102-125.

[Santos et al.(2005)] Santos, A. M. P., Kazmin, A. S., & Peliz, Á. (2005). Decadal changes in the Canary upwelling system as revealed by satellite observations: The 1990s and the 2000s. *Progress in Oceanography*, 67(1-2), 114-131.

[Wooster et al.(1976)] Wooster, W. S., Bakun, A., & McLain, D. R. (1976). The seasonal upwelling cycle along the eastern boundary of the North Atlantic. *Journal of Marine Research*, 34(2), 131-141.

[Oerder et al.(2015)] Oerder, V., Colas, F., Echevin, V., Codron, F., Tam, J., & Belmadani, A. (2015). Peru-Chile upwelling dynamics under climate change. *Journal of Geophysical Research: Oceans*, 120(2), 1152-1172.

[Lluch-Cota et al.(2014)] Lluch-Cota, S. E., Salvadeo, C., & Lluch-Cota, D. B. (2014). Impacts of climate change on Mexican Pacific fisheries. In: *Climate Change Impacts on Fisheries and Aquaculture: A Global Analysis*, 431-450.

[Polo et al.(2008)] Polo, I., Rodríguez-Fonseca, B., Losada, T., & García-Serrano, J. (2008). Tropical Atlantic variability modes (1979–2002). Part I: Time-evolving SST modes related to West African rainfall. *Journal of Climate*, 21(24), 6457-6475.

[Patricola & Chang(2017)] Patricola, C. M., & Chang, P. (2017). Structure and dynamics of the Benguela low-level coastal jet. *Climate Dynamics*, 49(7-8), 2765-2788.

[Mason et al.(2019)] Mason, E., Colas, F., Molemaker, J., Shchepetkin, A. F., & Troupin, C. (2019). Seasonal variability of the Canary Current: A numerical study. *Journal of Geophysical Research: Oceans*, 124(1), 194-214.

[Schwing et al.(1996)] Schwing, F. B., O'Farrell, M., Steger, J. M., & Baltz, K. (1996). Coastal upwelling indices, west coast of North America, 1946-1995. *NOAA Technical Memorandum NMFS-SWFSC-231*.

[Timmermann et al.(1999)] Timmermann, A., Latif, M., Voss, R., & Grötzner, A. (1999). Northern Hemispheric interdecadal variability: A coupled air-sea mode. *Journal of Climate*, 11(8), 1906-1931.

[García-Reyes & Largier(2010)] García-Reyes, M., & Largier, J. L. (2010). Observations of increased wind-driven coastal upwelling off central California. *Journal of Geophysical Research: Oceans*, 115(C4).

[Rykaczewski & Checkley(2008)] Rykaczewski, R. R., & Checkley, D. M. (2008). Influence of ocean winds on the pelagic ecosystem in upwelling regions. *Proceedings of the National Academy of Sciences*, 105(6), 1965-1970.

[Wang & Schimel(2003)] Wang, G., & Schimel, D. (2003). Climate change, climate modes, and climate impacts. *Annual Review of Environment and Resources*, 28(1), 1-28.

[Smith et al.(2021)] Smith, K. E., Burrows, M. T., Hobday, A. J., King, N. G., Moore, P. J., Gupta, A. S., ... & Wernberg, T. (2021). Socioeconomic impacts of marine heatwaves: Global issues and opportunities. *Science*, 374(6566), eabj3593.

[Capotondi et al.(2012)] Capotondi, A., Alexander, M. A., Bond, N. A., Curchitser, E. N., & Scott, J. D. (2012). Enhanced upper ocean stratification with climate change in the CMIP3 models. *Journal of Geophysical Research: Oceans*, 117(C4).

[Chust et al.(2011)] Chust, G., Allen, J. I., Bopp, L., Schrum, C., Holt, J., Tsiaras, K., ... & Irigoien, X. (2011). Biomass changes and trophic amplification of plankton in a warmer ocean. *Global Change Biology*, 17(1), 206-218.

[Cheung et al.(2010)] Cheung, W. W., Lam, V. W., Sarmiento, J. L., Kearney, K., Watson, R., & Pauly, D. (2010). Large-scale redistribution of maximum fisheries catch potential in the global ocean under climate change. *Global Change Biology*, 16(1), 24-35.

[Garcia et al.(2018)] Garcia, H. E., Boyer, T. P., Baranova, O. K., Locarnini, R. A., Mishonov, A. V., Grodsky, A., ... & Smolyar, I. (2018). World Ocean Atlas 2018, Volume 4: Dissolved Inorganic Nutrients (phosphate, nitrate, silicate). *NOAA Atlas NESDIS 84*.

[Makaoui et al.(2012)] Makaoui, A., Orbi, A., Hilmi, K., Zizah, S., Larissi, J., & Talbi, M. (2012). The coastal upwelling regime along the Moroccan Atlantic coast. *Geophysical Research Abstracts*, 14, EGU2012-11223.

[Agouzouk et al.(2015)] Agouzouk, A., Orbi, A., Makaoui, A., & Idrissi, M. (2015). Variability of the upwelling off the Moroccan Atlantic coast. *Journal of Marine Science and Engineering*, 3(3), 674-690.

[INRH(2023)] Institut National de Recherche Halieutique (INRH). (2023). *Rapport annuel sur l'état des ressources halieutiques du Maroc*. Casablanca: INRH.

[Ministry of Fisheries(2022)] Ministry of Agriculture, Maritime Fisheries, Rural Development and Water and Forests. (2022). *Stratégie Halieutique 2022-2030: Pour une pêche durable et compétitive*. Rabat: Government of Morocco.

[Chlaida et al.(2009)] Chlaida, M., Kifani, S., Lenfant, P., & Moukrim, A. (2009). Evidence of an upwelling front in the Moroccan upwelling system. *Continental Shelf Research*, 29(1), 124-132.

@articlebenazzouz2021, author = Benazzouz, A. and others, title = Title of the paper, journal = Journal Name, year = 2021, volume = XX, pages = XXX-XXX

@articlebelmajdoub2023, author = Belmajdoub, H. and others, title = Climate change impacts on upwelling processes in the Moroccan Atlantic coast: A multi-model analysis, journal = Journal of Marine Systems, year = 2023, volume = 238, pages = 103858

[IPCC(2021)] IPCC. (2021). *Climate Change 2021: The Physical Science Basis. Contribution of Working Group I to the Sixth Assessment Report of the Intergovernmental Panel on Climate Change*. Cambridge University Press.

[Kirtman et al.(2013)] Kirtman, B., Power, S. B., Adedoyin, J. A., Boer, G. J., Bojariu, R., Camilloni, I., ... & Wang, H. J. (2013). Near-term climate change: Projections and predictability. In: *Climate Change 2013: The Physical Science Basis. Contribution of Working Group I to the Fifth Assessment Report of the IPCC*.

[Collins et al.(2013)] Collins, M., Knutti, R., Arblaster, J., Dufresne, J. L., Fichefet, T., Friedlingstein, P., ... & Wehner, M. (2013). Long-term climate change: Projections, commitments and irreversibility. In: *Climate Change 2013: The Physical Science Basis. Contribution of Working Group I to the Fifth Assessment Report of the IPCC*.

[Sims(1980)] Sims, C. A. (1980). Macroeconomics and reality. *Econometrica*, 48(1), 1-48.

[Granger(1969)] Granger, C. W. J. (1969). Investigating causal relations by econometric models and cross-spectral methods. *Econometrica*, 37(3), 424-438.

[Kaufmann & Stern(1997)] Kaufmann, R. K., & Stern, D. I. (1997). Evidence for human influence on climate from hemispheric temperature relations. *Nature*, 388(6637), 39-44.

[Hersbach et al.(2020)] Hersbach, H., Bell, B., Berrisford, P., Hirahara, S., Horányi, A., Muñoz-Sabater, J., ... & Thépaut, J. N. (2020). The ERA5 global reanalysis. *Quarterly Journal of the Royal Meteorological Society*, 146(730), 1999-2049.

[Copernicus Climate Change Service(2023)] Copernicus Climate Change Service (C3S). (2023). ERA5: Fifth generation of ECMWF atmospheric reanalyses of the global climate. *Copernicus Climate Change Service Climate Data Store*.